IOPscience iopscience.iop.org

Home Search Collections Journals About Contact us My IOPscience

Application of curved-wavefront approximations to multiple-scattering effects in EXAFS of ReO_3

This article has been downloaded from IOPscience. Please scroll down to see the full text article.

1989 J. Phys.: Condens. Matter 1 7715

(http://iopscience.iop.org/0953-8984/1/41/024)

View the table of contents for this issue, or go to the journal homepage for more

Download details:
IP Address: 171.66.16.96
The article was downloaded on 10/05/2010 at 20:33

Please note that terms and conditions apply.

J. Phys.: Condens. Matter **1** (1989) 7715–7721. Printed in the UK

Application of curved-wavefront approximations to multiple-scattering effects in EXAFS of ReO_3

V Fritzsche

Sektion Physik, Technische Universität Dresden, Mommsenstrasse 13, DDR-8027 Dresden, German Democratic Republic

Received 7 October 1988, in final form 5 April 1989

Abstract. Multiple-scattering effects in EXAFS of the rhenium L_3 edge are calculated with the reduced angular momentum expansion (RAME) and with the modified small-scattering-centre approximation (MSSCA). The multiple-scattering enhancement in the nearly collinear Re–O–Re bonds is very sensitive to changes in the bond angle. A comparison of the theoretical results with the pressure-dependent measurements of Alberding *et al* (1986) confirms the relation between the pressure and the bond angle that follows from the structure model of Jørgensen *et al* (1986) for the high-pressure phases in ReO_3.

1. Introduction

In the last decade several studies of the high-pressure phases in ReO_3 have been published (Jørgensen *et al* 1986 and references therein). At atmospheric pressure ReO_3 has a non-distorted perovskite structure. In the high-pressure phase above 5.0 kbar the ReO_6 octahedra are rotated as rigid units. The angle of rotation is an order parameter for the phase transition and varies as $(P - P_c)^{\delta}$ with $\delta = 0.322$ (Jørgensen *et al* 1986). Thereby the bonds Re–O–Re are buckled and the bond angle is continuously changed with pressure.

Recently, Alberding *et al* (1986) have measured EXAFS of the rhenium L_3 edge as a function of the pressure. They found that the height of the first rhenium peak in the Fourier transform depends strongly on the pressure due to multiple-scattering processes at the oxygen atom 3 which lies between the absorbing rhenium atom 1 and the back-scattering rhenium atom 2 (figure 1). The forward-scattering processes at the intervening oxygen atom give rise to a considerable enhancement of the EXAFS contributions from these chains, which, however, drops off rapidly as the angle β increases. As shown by Teo (1981) this effect can be used for angle determinations.

It is generally acknowledged now that the plane-wave approximation (PWA), commonly applied in the theoretical approach for EXAFS, is only justified for backscattering processes (Barton and Shirley 1985b, c, Poon *et al* 1986). In nearly collinear chains of atoms, where forward-scattering processes play an important role, spherical-wave effects must therefore be included in the calculations. The present paper reports theoretical results obtained with the reduced angular momentum expansion (RAME) and with the modified small-scattering-centre approximation (MSSCA) (Fritzsche and Rennert 1986, Fritzsche 1988).

0953-8984/89/417715 + 07 $02.50 © 1989 IOP Publishing Ltd

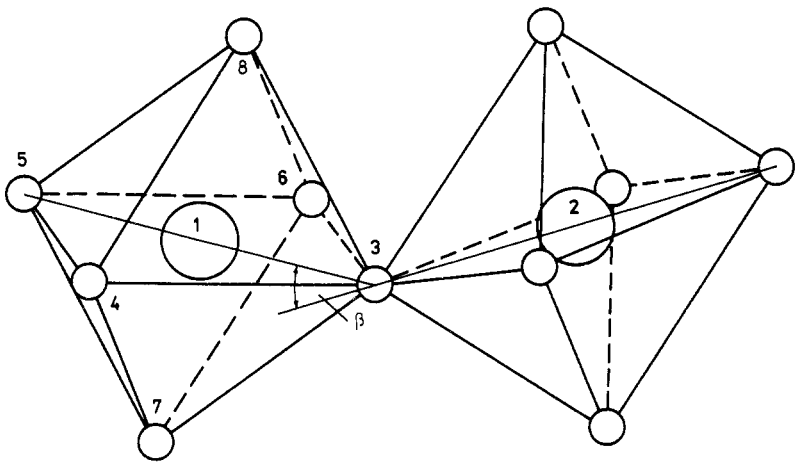

Figure 1. Structure model for the high-pressure phase in ReO_3. The rhenium atoms are depicted as big circles and the oxygen atoms as small ones.

2. Theory

For polycrystalline samples the EXAFS function is given by (Lee and Pendry 1975, Gurman *et al* 1986)

$$\chi(k) = \frac{1}{2l+1}\,\mathrm{Re}[\exp(2\mathrm{i}\,\delta_l')\sum_m Z_{LL}] \tag{1}$$

where $L = (l, m)$. k is the wavenumber of the excited electrons and $l = l_0 + 1$ is determined by the angular momentum of the initial state l_0. The outgoing waves to $l = l_0 - 1$ are neglected. The matrix Z_{LL}, describes the scattering processes of the electrons in the final state. It may be written as a sum over all closed loops starting and terminating at the absorbing atom $\boldsymbol{R}_1$

$$Z_{LL'} = \sum_{\boldsymbol{R}_2}{}' \sum_{L_2} G_{LL_2}(\boldsymbol{R}_{12}) T_{l_2}(\boldsymbol{R}_2) G_{L_2L'}(\boldsymbol{R}_{21}) + \sum_{\boldsymbol{R}_2\boldsymbol{R}_3} \sum_{L_2L_3} \times G_{LL_3}(\boldsymbol{R}_{13}) T_{l_3}(\boldsymbol{R}_3) G_{L_3L_2}(\boldsymbol{R}_{32}) T_{l_2}(\boldsymbol{R}_2) G_{L_2L'}(\boldsymbol{R}_{21}) + \ldots, \tag{2}$$

with $\boldsymbol{R}_{ij} = \boldsymbol{R}_i - \boldsymbol{R}_j$ and $T_l(\boldsymbol{R}_j) = \mathrm{i}\sin\delta_l \exp(\mathrm{i}\,\delta_l)$, where δ_l are the scattering phase shifts of the atom $\boldsymbol{R}_j$. All terms containing an $\boldsymbol{R}_{ij} = \boldsymbol{0}$ are excluded from the summations in (2).

The coefficients $G_{LL'}(\boldsymbol{R}_{ij})$ describe the free electron propagator in a two-centre angular momentum representation. In the MSSCA (Fritzsche 1988) these coefficients are approximated by

$$G_{LL'}(\boldsymbol{R}) \approx 4\pi \frac{\mathrm{i}^{l-l'}}{\mathrm{i}kR} \exp[\mathrm{i}kR + \mathrm{i}a_l(kR) + \mathrm{i}a_{l'}(kR)] Y_L^*(\boldsymbol{R}) Y_{L'}(\boldsymbol{R}) \tag{3}$$

with

$$a_l(x) = l(l+1)/2x. \tag{4}$$

Then the sums over L_2, L_3 etc in $Z_{LL'}$ can be written as effective-scattering amplitudes (Fritzsche and Rennert 1987). In this approach the incident spherical electron waves are

represented near the scattering potential by isotropic spherical waves. Furthermore all spherical Hankel functions are approximated by

$$h_l(x) \approx \mathrm{i}^{-l} h_0(x) \exp[\mathrm{i} a_l(x)]. \tag{5}$$

The small-atom approximation of Lee and Pendry (1975), which was recently applied by Pettifer *et al* (1986) and Gurman (1988), corresponds to the case that only $a_{l'}(kR)$ is included in (3), whereas $a_l(kR)$ is neglected. Setting both $a_l(kR) = 0$ and $a_{l'}(kR) = 0$ one obtains the commonly used PWA.

In the more sophisticated RAME (Fritzsche and Rennert 1986) the incident electron waves are approximated in the range of the scattering potential by a set of spherical waves with the lowest angular momenta $L = \{(0, 0); (1, 1); (1, 0); (1, -1)\}$. In this way both the curvature and the anisotropy of the incident wave are taken into account. Then the coefficients for vectors on the positive z axis,

$$G_{LL'}(R\boldsymbol{e}_z) = g_{ll'm}(R)\delta_{mm'} \tag{6}$$

are given by (Fritzsche 1988)

$$g_{ll'm}(R) \approx [(2l+1)(2l'+1)]^{1/2}(\mathrm{i}^{l-l'}/\mathrm{i}kR) \times \exp(\mathrm{i}kR + \mathrm{i}a_l(kR) + \mathrm{i}a_{l'}(kR))$$
$$\times [(1 - a_l(kR)a_{l'}(kR))\delta_{m,0} - \mathrm{i}(a_l(kR)a_{l'}(kR))^{1/2}\delta_{m,\pm 1}]. \tag{7}$$

Similar formulae were published by Rehr *et al* (1986).

The coefficients $G_{LL'}(\boldsymbol{R})$ corresponding to arbitrary vectors $\boldsymbol{R}$ can be constructed from (7) using rotations of the coordinate system. Then rotation matrices appear in $Z_{LL'}$ that describe the rotation of a coordinate system with the z axis $\boldsymbol{R}$ into a system with the z axis $\boldsymbol{R}'$

$$D^{(l)}_{mm'}(\boldsymbol{R}', \boldsymbol{R}) = \mathrm{e}^{\mathrm{i}m\gamma}\, d^{(l)}_{mm'}(\beta)\, \mathrm{e}^{\mathrm{i}m'\alpha} \tag{8}$$

where α, β and γ are the appropriate Eulerian angles.

Finally one obtains

$$\sum_m Z_{LL} = \sum_{\boldsymbol{R}_2}{}' \sum_{l_2} \sum_{q_1} (g_{ll_2q_1}(R_{12}) d^{(0)}_{00}(\pi))^2 T_{l_2}(\boldsymbol{R}_2)$$
$$+ \sum_{\boldsymbol{R}_2\boldsymbol{R}_3}{}' \sum_{l_2 l_3} \sum_{q_1 q_2 q_3} D^{(l)}_{q_1 q_3}(\boldsymbol{R}_{21}, \boldsymbol{R}_{13}) g_{ll_3q_3}(R_{13}) D^{(l_3)}_{q_3 q_2}(\boldsymbol{R}_{13}, \boldsymbol{R}_{32})$$
$$\times T_{l_3}(\boldsymbol{R}_3) g_{l_3 l_2 q_2}(R_{32}) D^{(l_2)}_{q_2 q_1}(\boldsymbol{R}_{32}, \boldsymbol{R}_{21})$$
$$\times T_{l_2}(\boldsymbol{R}_2) g_{l_2 l q_1}(R_{21}) + \ldots. \tag{9}$$

The first term in this series describes the single-scattering contributions, the second one the double-scattering loops etc. Because of (7) the magnetic quantum numbers q_1, q_2 etc are restricted to the low values -1, 0 and $+1$, for which the rotation matrices are given by

$$d^{(l)}_{0,0} = P_l(\cos\beta)$$
$$d^{(l)}_{\pm 1,0} = d^{(l)}_{0,\mp 1} = \pm [l/(l+1)]^{1/2} [P_{l-1}(\cos\beta) - \cos\beta\, P_l(\cos\beta)]/\sin\beta \tag{10}$$
$$d^{(l)}_{1,\pm 1} = d^{(l)}_{-1,\mp 1} = [P_{l-1}(\cos\beta) - (\cos\beta \mp 1)P_l(\cos\beta) + P_{l+1}(\cos\beta)]/(1 \pm \cos\beta)$$

where $P_l(x)$ are the Legendre polynomials.

Inelastic scattering processes are described by exponential damping terms in the $g_{ll'm}$

$$g_{ll'm}(R) \rightarrow g_{ll'm}(R)\, e^{-R/(2\lambda)} \tag{11}$$

where λ is the electron mean free path. Thermal vibrations are included by appropriate Debye–Waller factors, which are incorporated in the rotation matrices. In this way the motions of both the absorbing and the scattering atoms are taken into account. For uncorrelated and isotropic vibrations one obtains

$$d^{(l)}_{mm'}(\beta) \rightarrow d^{(l)}_{mm'}(\beta) \exp(-k^2 u_i^2 (1-\cos\beta)) \tag{12}$$

where u_i^2 is the mean square displacement of the atom considered.

3. Results and discussion

Teo (1981) has included the effects of multiple-scattering processes by an amplitude factor Ω and a phase shift ω in the single-scattering expression for EXAFS. By means of Ω and ω one takes into account all multiple-scattering loops that have the same length as the direct backscattering process and that therefore contribute to the same peak in the Fourier transform of $\chi(k)$. In the framework given above they are defined by

$$\Omega\, e^{i\omega} = \sum_m Z^{MS}_{LL}(2R_{12}) \Big/ \sum_m Z^{SS}_{LL}(2R_{12}) \tag{13}$$

where $Z^{SS}_{LL}(2R_{12})$ describes the single-scattering contribution $1 \rightarrow 2 \rightarrow 1$, whereas $Z^{MS}_{LL}(2R_{12})$ contains all multiple-scattering loops (including $1 \rightarrow 2 \rightarrow 1$) which have the same path length $2R_{12}$ (figure 1).

We have calculated Ω and ω as a function of β (figure 1) and k for the first rhenium peak in the Fourier transform of the rhenium L_3 edge EXAFS with the above-mentioned approximations. In figure 2 the amplitude factor Ω is shown for the atoms 1, 2 and 3 which are arranged in an approximately collinear array (figure 1). All the included pathways ($1 \rightarrow 2 \rightarrow 1$, $1 \rightarrow 2 \rightarrow 3 \rightarrow 1$, $1 \rightarrow 3 \rightarrow 2 \rightarrow 1$, and $1 \rightarrow 3 \rightarrow 2 \rightarrow 3 \rightarrow 1$) contain one backscattering event at the rhenium atom 2. For the highly symmetric geometry at $\beta = 0°$ the approximations can be compared to a full partial wave calculation. The good agreement between the RAME and these exact results confirms that this approximation is adequate to the considered problem. Also the deviations of the MSSCA from the exact values seem to be unimportant for the total Ω shown in figure 2, but for selected scattering pathways the errors of the MSSCA are larger. For example, for the scattering loop $1 \rightarrow 3 \rightarrow 2 \rightarrow 3 \rightarrow 1$, which contains two forward scattering processes, the ratio $\Omega_{MSSCA}/\Omega_{exact}$ amounts to about 1.3 at $\beta = 0°$. The large errors of the PWA demonstrate convincingly the importance of curved-wavefront corrections and explain why the PWA results of Alberding *et al* (1986) are in poor agreement with the experimental data.

Figure 1 illustrates that further scattering loops with the same path length $2R_{12}$ exist in the octahedron around the absorbing atom 1. These additional scattering pathways contain two backscattering events at the oxygen atoms in the corners of the octahedron. Figure 3 shows that their contribution to Ω is negligible for low angles β. The most important of them is the third-order process $1 \rightarrow 3 \rightarrow 1 \rightarrow 5 \rightarrow 1$ by reason of the strong forward scattering effect at the absorbing rhenium atom 1.

In figure 4 the theoretical results for Ω and ω are compared with experimental values from Alberding *et al* (1986). The relation between the pressure and the angle β was

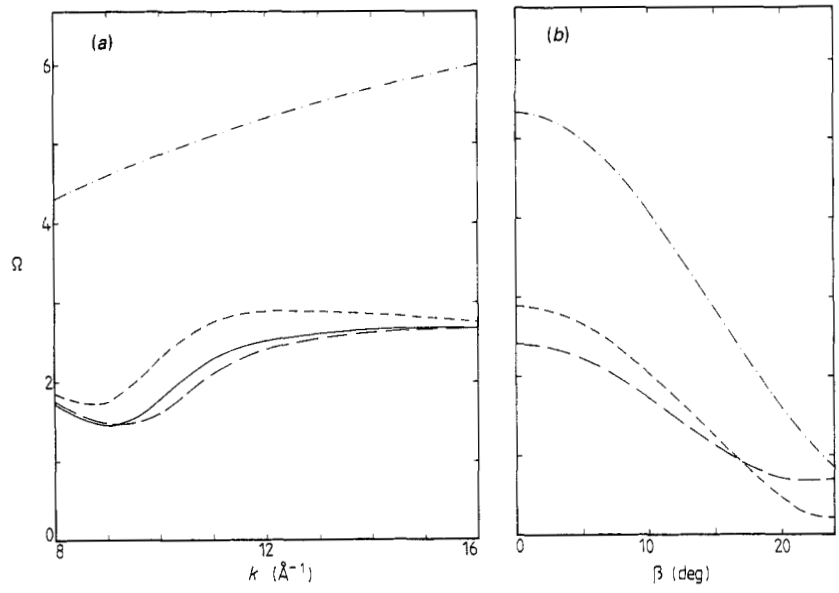

Figure 2. Multiple-scattering enhancement Ω in the chain of the atoms 1, 2 and 3 calculated with a full partial wave expansion (solid line), with the RAME (long-dashed line), with the MSSCA (short-dashed line), and with the PWA (chained line) (*a*) for $\beta = 0°$ and (*b*) for $k = 12$ Å^{-1}. The Debye–Waller factors were neglected.

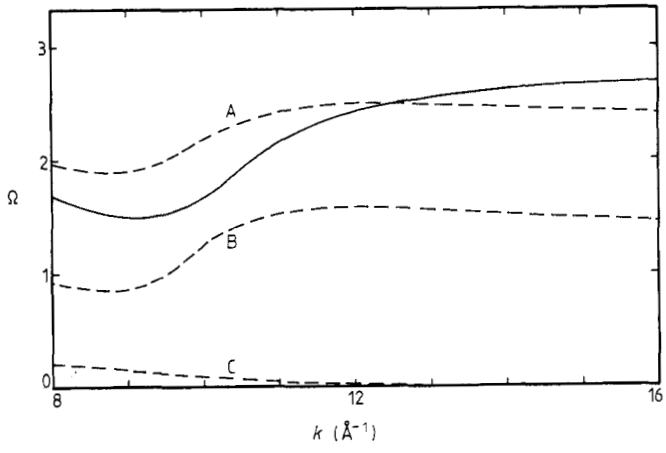

Figure 3. Multiple-scattering enhancement Ω including all scattering loops with the length $2R_{12}$ (solid line) and contributions from selected scattering pathways (dashed lines) for $\beta = 0°$ in the RAME: (A) contribution of the double-scattering loops $1 \rightarrow 2 \rightarrow 3 \rightarrow 1$ and $1 \rightarrow 3 \rightarrow 2 \rightarrow 1$; (B) contribution of the triple-scattering loop $1 \rightarrow 3 \rightarrow 2 \rightarrow 3 \rightarrow 1$; (C) contribution of the triple-scattering loop $1 \rightarrow 3 \rightarrow 1 \rightarrow 5 \rightarrow 1$. The Debye–Waller factors were neglected.

newly calculated from the structural data given by Jørgensen *et al* (1986). The mean square displacements for the Debye–Waller factors were taken from the neutron powder diffraction measurements of Jørgensen *et al* (1986) assuming an uncorrelated motion of the atoms. Within these model assumptions the effect of the thermal vibrations on Ω

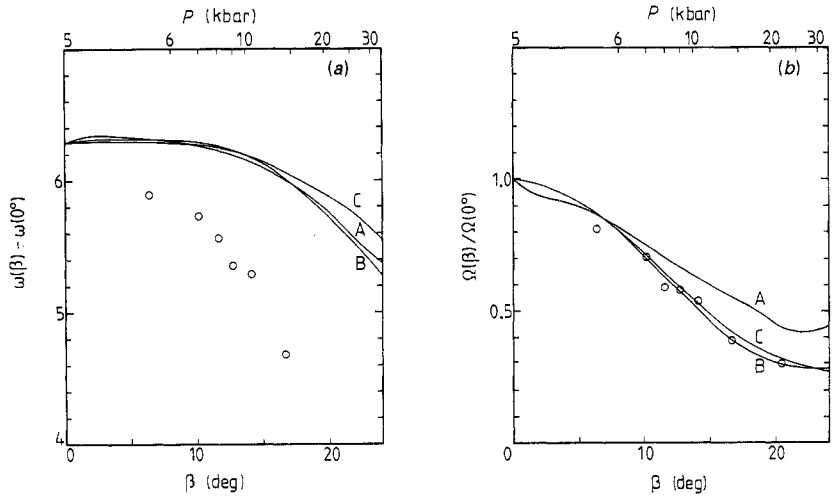

Figure 4. (*a*) Ratio $\Omega(\beta)/\Omega(\beta = 0°)$ and (*b*) phase difference $\omega(\beta)-\omega(\beta = 0°)$ calculated with the RAME (including the Debye–Waller factors). (A) $k = 8$ Å^{-1}; (B) $k = 12$ Å^{-1}; and (C) $k = 16$ Å^{-1}. The experimental values (circles) from Alberding *et al* (1986) are taken at $k = 12$ Å^{-1}.

and ω is negligible, because the prevailing scattering pathways differ from each other only in the number of forward-scattering processes, for which the influence of lattice vibrations is small according to (12). The only influence of the Debye–Waller factors is to diminish the contributions from the scattering pathways which include two back-scattering processes. Figure 4 shows that the experimental values for $k = 12$ Å^{-1} are well described by the calculations. This confirms unambiguously the buckling of the Re–O–Re chain in the high-pressure phase of ReO_3. In particular, the quantitative agreement of the calculated values for Ω with the experimental data corroborates the relation between the rotation angle of the octahedra and the pressure, which was derived from the neutron powder diffraction data by Jørgensen *et al* (1986). The systematic variations of the experimental curves as a function of the wavenumber k are not reproduced by the calculations. Probably, these changes in the data of Alberding *et al* (1986) are an effect of the Fourier transform technique, because Fourier filtering systematically distorts the structures for the lower and upper wavenumbers (Lee *et al* 1981).

4. Conclusions

We have presented an efficient multiple-scattering expression for EXAFS and XANES based on the RAME. This approximation takes into account both the curvature and the anisotropy of the spherical waves. The formulae derived are much simpler and computationally faster than the exact multiple-scattering expression (Gurman *et al* 1986). In the Taylor-series magnetic-quantum-number expansion of Barton and Shirley (1985a, c) the formula for the coefficients $g_{ll'm}(R)$ is much more complicated than the expression in the RAME (7). For the energies considered one has to calculate a lot of terms in their double sum for the $g_{ll'm}(R)$ in order to attain the same accuracy as the RAME.

It can be concluded that the RAME and, to a certain extent the MSSCA also, are appropriate methods to include spherical-wave effects in multiple-scattering calculations of EXAFS. This was also confirmed by Rennert and Hung (1988).

The presented theoretical results for the rhenium L_3 edge EXAFS support the structure model of Jørgensen *et al* (1986) for the high-pressure phases in ReO_3.

Acknowledgments

The author is grateful to Dr G Seifert for assistance in obtaining the scattering phase shifts.

References

Alberding N, Crozier E D, Ingalls R and Houser B 1986 *J. Physique Coll.* **47** C8 681–4
Barton J J and Shirley D A 1985a *Phys. Rev.* A **32** 1019–26
—— 1985b *Phys. Rev.* B **32** 1892–905
—— 1985c *Phys. Rev.* B **32** 1906–20
Fritzsche V 1988 *Phys. Status Solidi* b **147** 485–94
Fritzsche V and Rennert P 1986 *Phys. Status Solidi* b **135** 49–60
—— 1987 *Phys. Status Solidi* b **142** 15–25
Gurman S J 1988 *J. Phys. C: Solid State Phys.* **21** 3699–717
Gurman S J, Binsted N and Ross I 1986 *J. Phys. C: Solid State Phys.* **19** 1845–61
Jørgensen J-E, Jorgensen J D, Batlogg B, Remeika J P and Axe J D 1986 *Phys. Rev.* B **33** 4793–8
Lee P A, Citrin P H, Eisenberger P and Kincaid B M 1981 *Rev. Mod. Phys.* **53** 769–806
Lee P A and Pendry J B 1975 *Phys. Rev.* B **11** 2795–811
Pettifer R F, Foulis D L and Hermes C 1986 *J. Physique Coll.* **47** C8 545–50
Poon H C, Snider D and Tong S Y 1986 *Phys. Rev.* B **33** 2198–206
Rehr J J, Albers R C, Natoli C R and Stern E A 1986 *Phys. Rev.* B **34** 4350–3
Rennert P and Hung N V 1988 *Phys. Status Solidi* b **148** 49–61
Teo B-K 1981 *J. Am. Chem. Soc.* **103** 3990–4001